

**Supplemental material for: Observing the quantum wave nature of free electrons through spontaneous emission**

Roei Remez,<sup>1,\*</sup> Aviv Karnieli,<sup>1,□</sup> Sivan Trajtenberg-Mills,<sup>1</sup> Niv Shapira,<sup>1</sup> Ido Kaminer,<sup>2</sup>  
Yossi Lereah,<sup>1</sup> and Ady Arie<sup>1</sup>

<sup>1</sup>*School of Electrical Engineering, Fleischman Faculty of Engineering, Tel Aviv University, Tel Aviv, Israel*

<sup>2</sup>*Department of Electrical Engineering, Technion–Israel Institute of Technology, Haifa 32000, Israel*

□ These authors contributed equally

\*Corresponding author: roei.remez@gmail.com

**A. Experimental details and electron beam characteristics**

We used Thorlabs GH13-24U holographic grating for the experiment, which is a silver grating on a dielectric substrate with a period of 416nm. For each of the two electron beams (wide and narrow) and for each angle  $\phi$ , an image of the grating was acquired. For each image, the gray levels of the SPR area were summed, and a DC level was subtracted according to the dark region of the grating close to the radiation area. Since the camera had constant gain and the aperture of the optical system was constant throughout the experiment, this summation is proportional to the emitted radiation power per steradian around angle  $\phi$ . The values were then corrected for Fresnel refractions from both surfaces of the viewing chamber and divided by  $\cos \phi$  to account for the projection of the radiated area on the observation angle.

In the narrow beam experiment, the electron wavefront was focused to a point. At the focal point, assuming negligible aberrations, the phase of the electron wavefunction is flat. For the wide beam, only one of the axes is focused, while the other is defocused, creating an elliptical shape. Here we show that the long axis of the beam has negligible divergence because of the extremely small convergence semi-angle in the viewing chamber area. Consider the setup shown in figure S1, which shows the two different axes of the astigmatic beam.

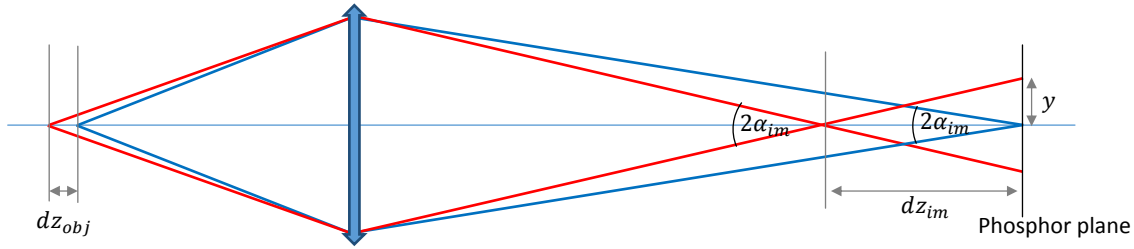


Figure S1: In blue – focused stigmatic beam and the focused axis of the astigmatic beam. In red – the diverged (elongated) axis of the astigmatic beam.

The magnification value  $M$  is the ratio between the electron beam spot size (when focused) at the phosphore screen region and the beam spot size at the microscope’s “object plane”. We note that in our experiment the grating was placed close to the phosphor screen and the “object plane” of the microscope remained empty. The defocus value in the “object plane” area  $dz_{obj}$  and the magnification  $M$  are given by the microscope’s software.  $y$  is tuned using the stigmators to be approximately 1mm (in red) at the ruling’s direction, while the width at the other transverse axis remains the same (in blue). The sag (peak-to-valley of the wavefront equi-phase surfaces) is given by:

$$SAG = \frac{y^2}{2dz_{im}} = \frac{y^2}{2M^2 dz_{obj}} \quad (S1)$$

And the convergence semi-angle in the image:

$$\alpha_{im} \approx \frac{y}{dz_{im}} = \frac{y}{M^2 dz_{obj}} \quad (S2)$$

For the parameters of our experiment,  $y \approx 1mm$ ,  $M=1850$ ,  $dz_{obj} = 0.8mm$ , we get  $SAG = 0.18 nm$ , and  $\alpha_{im} = 0.36 \mu rad$ . In our experiments, the grating period is 416nm and interaction length is about  $10 \mu m$ , therefore the SAG is more than three orders of magnitude smaller than the grating period, and 4 orders of magnitude smaller than the interaction length. Therefore, the divergence of the elongated axis of the beam is negligible, and the phase is approximately flat. In addition, the effect of the astigmatism is at least an order of magnitude larger than other aberrations, and therefore the contribution of other aberrations to the astigmatic SAG value is negligible.

### B. Electron beam transverse coherence

In this section we detail the measurements and analysis done in order to verify that the wide electron beam's transverse coherence length (TCL) at the grating plane is significantly wider than the emitted wavelength, thus meeting the theoretical assumptions used in this work.

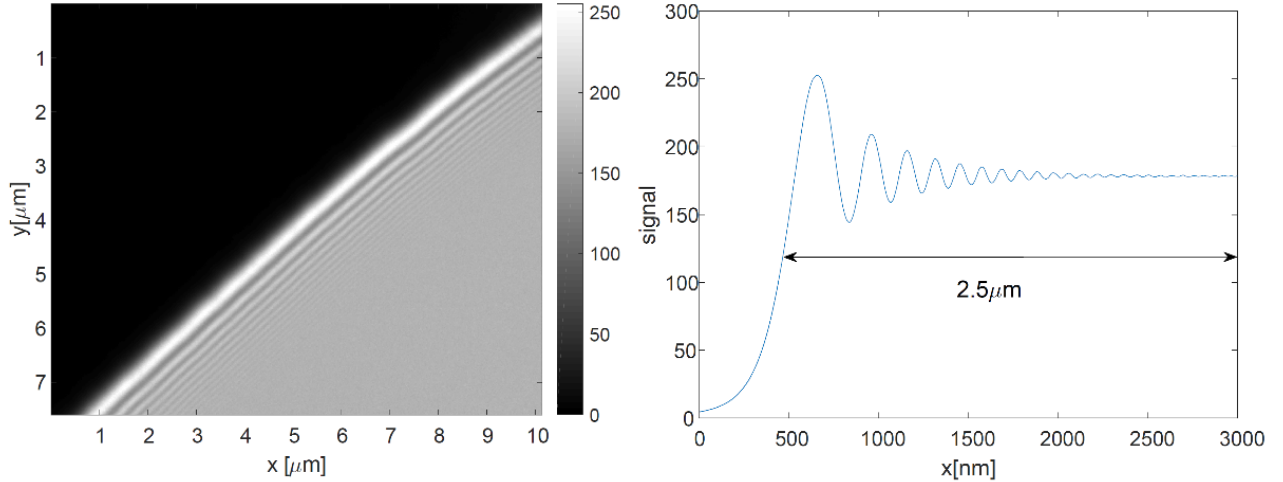


**Figure S2: (a) Observed Fresnel fringes at the limiting aperture plane. (b) Averaged signal of the aperture edge, demonstrating a  $2.5 \mu m$  range of resolvable fringes.**

Both experimentally and theoretically, that FEGs are partially coherent sources [4–7], where, using a biprism, TCLs exceeding a millimeter were measured in low current densities. Further, holograms of tens of microns in size were reported in [5–7]. Therefore, we generally expect the TCL in parallel illumination mode, to obtain large values exceeding a few microns (depending strongly on the working conditions, and particularly on the current density and extraction field of the FEG).

In spite of the biprism interference method being the preferable and most straightforward technique of measuring the TCL [1,8], the apparatus can be damaged in high current densities. On the other hand, the latter are needed in order to maintain high SNR for the optical radiation in the experiment. Therefore, in order to measure the TCL in the respective working conditions, we resorted to the Fresnel fringes method [1,9], wherein the near-field diffraction of the beam from an opaque edge is measured in defocus. In the limit of small defocus relative to the distance to the source, the lateral extent of resolvable fringes from the edge position provides a lower-bound estimate for the TCL [9]. The method is mainly limited by

SNR of the TEM image, as the fringes' contrast inherently decays away from the edge. Using this method, we measured a TCL of 2.5  $\mu\text{m}$  at the limiting aperture's plane, near the second condenser lens, of diameter 150  $\mu\text{m}$ . The measurement results are displayed in Fig. S2.

In Ref. [10], it was proven that for an electron-optical system comprising lenses and apertures, the ratio of the TCL to the beam size is a constant along the beam propagation in the system. This constant, called the coherence parameter [10] or beam parameter [2,4], is related to the beam's 'etendue' [10], which is also a conserved quantity. We use this observation to determine a lower bound to the TCL in the grating plane, using the measured beam size, and the TCL (2.5  $\mu\text{m}$ ) and aperture diameter (150  $\mu\text{m}$ ) in the plane where the Fresnel fringes were observed. The coherence parameter was found to be  $K = 0.0167$ , a relatively small fraction of the beam lateral width, due to the non-ideal working conditions of high current density and largest possible limiting aperture (necessary for high optical SNR, as discussed above). However, as we increase the beam lateral size at the grating plane, the lower bound for the TCL takes a satisfactory value of

$$\text{TCL} \geq \begin{cases} 5 \mu\text{m}, & \text{narrow beam of } 300 \mu\text{m} \\ 33 \mu\text{m}, & \text{wide beam of } 2000 \mu\text{m} \end{cases}$$

being at least more than 60 times larger than the optical wavelength for the case of the wide beam. This result is in accordance with the assumptions employed in the theoretical derivation, wherein the wavefunction coherence is assumed much larger than the optical wavelength.

### C. Detailed QED derivation

We combine the approaches of Ref [11] for solving the Dirac Hamiltonian and the electromagnetic Bloch-modes approach of Ref [12]. First, we consider an electron-photon state subject to the unperturbed Dirac Hamiltonian

$$H_0 = c\boldsymbol{\alpha} \cdot \mathbf{p} + \boldsymbol{\beta}mc^2 + \sum_{\mathbf{q},n\sigma} \hbar\omega_{\mathbf{q}n\sigma} a_{\mathbf{q}n\sigma}^\dagger a_{\mathbf{q}n\sigma} \quad (\text{S3})$$

where  $\boldsymbol{\alpha} = (\boldsymbol{\alpha}_1, \boldsymbol{\alpha}_2, \boldsymbol{\alpha}_3)$  and  $\boldsymbol{\beta}$  are the Dirac matrices,  $\mathbf{p} = -i\hbar\nabla$  the momentum operator and  $\omega_{\mathbf{q}n\sigma}, a_{\mathbf{q}n\sigma}$  are the frequency and annihilation operator of the electromagnetic field, where  $\sigma = 1,2$  are the two polarizations and  $n$  is the band index. The unperturbed Hamiltonian takes into account the boundary conditions imposed by the periodic grating. The latter imply that the eigenmodes of the electromagnetic field must be given as periodic functions along the direction of the grating periodicity,  $\Lambda$ ,

$$\mathbf{A} = \sum_{\mathbf{q},n,\sigma} \sqrt{\frac{\hbar}{2\epsilon_0 V \omega_{\mathbf{q},n,\sigma}}} \left[ a_{\mathbf{q},n,\sigma} \sum_{m=-\infty}^{\infty} \boldsymbol{\epsilon}_{m,\mathbf{q}n\sigma}(\mathbf{r}_T) A_{m,\mathbf{q}n\sigma}(\mathbf{r}_T) e^{i\mathbf{q}_m \cdot \mathbf{r}} + c. c. \right] \quad (\text{S4})$$

where  $\mathbf{q}_m = (q_x, q_{ym}, q_z + \kappa_m)$ , with  $q_{ym} = \sqrt{q^2 - (q_z + \kappa_m)^2 - q_x^2}$ ,  $\kappa_m = m \frac{2\pi}{\Lambda}$ ,  $\epsilon_0$  the vacuum permittivity,  $V$  the quantization volume and  $\boldsymbol{\epsilon}_{m,\mathbf{q}n\sigma}$  is the field polarization vector of the  $m$ -th component, which is dependent on the details of the boundary. The  $A_{m,\mathbf{q}n\sigma}$  coefficients satisfy a normalization condition  $\sum_m \int d^2x |A_{m,\mathbf{q}\sigma}|^2 = 1$ . In the most general case, we allow for the mode coefficients and polarization to vary along the transverse coordinates  $\mathbf{r}_T = (x, y)$ .

This quantization scheme expands the electromagnetic field in modes  $\mathbf{q}n\sigma$ , each with an infinite number of  $\mathbf{q}_m$  in its corresponding Fourier series. For simplicity, we assume that only the  $m = 0$  term is

propagating ( $q_{ym}$  is real), while for  $m \neq 0$  it is evanescent in the  $y$  direction ( $q_{ym} = i\alpha_m$  is imaginary). This implies that momentum conservation is made possible through the evanescent parts of the mode, which contain the extra longitudinal momentum,  $q_z + \kappa_m$ , necessary for momentum conservation. When such a mode is excited, the generated surface waves stay in the near field, whereas the propagating part can be detected in the far field.

The interaction Hamiltonian is readily given by taking  $\mathbf{p} \rightarrow \mathbf{p} + e\mathbf{A}$  in the Dirac Hamiltonian, i.e.  $H_{\text{int}} = ec\boldsymbol{\alpha} \cdot \mathbf{A}$ , where  $e$  is the electron charge. We assume that the initial electron-photon state can be expressed as a superposition of free-space electron modes multiplied by the electromagnetic vacuum state

$$|\psi_i\rangle = \sum_{\mathbf{k}_i} \frac{1}{\sqrt{V}} \tilde{\psi}(\mathbf{k}_i) |\mathbf{k}_i \mathbf{s}_i; 0\rangle = |0\rangle \otimes \sum_{\mathbf{k}_i} \mathbf{u}_i(\mathbf{s}_i, \mathbf{k}_i) \frac{1}{\sqrt{V}} \tilde{\psi}(\mathbf{k}_i) |\mathbf{k}_i\rangle \quad (\text{S5})$$

Where  $\mathbf{k}_i = (k_{ix}, k_{iy}, k_{iz})$  is the initial wave-vector of the electron with a pure spin state  $\mathbf{s}_i$ ,  $\mathbf{u}$  is a 4-component spinor of the electron, and  $\tilde{\psi}(\mathbf{k}_i)$  is the spectral envelope of the electron wave function, sharply peaked near the carrier initial wave vector  $\mathbf{k}_{0i}$ . Having the sharp wave vector distribution is equivalent to a paraxial approximation around the axis  $\mathbf{k}_{0i}$ . Generally speaking, this paraxial electron envelope can be written as the product of a transverse wave function and a longitudinal wavefunction along the propagation axis  $z$ :

$$\tilde{\psi}(\mathbf{k}_i) = \tilde{\psi}_T(\mathbf{k}_{iT}) \tilde{\psi}_z(k_{iz}) \quad (\text{S6})$$

where  $\mathbf{k}_{iT} = (k_{ix}, k_{iy})$  is the transverse part of the initial wave vector  $\mathbf{k}_i$ .

The transition rate between the initial and final states can be calculated using a generalized version of the Fermi golden rule [7]. The latter is based on the first order time-dependent perturbation expansion of the state evolution, and on the realization that the transition rate to a state with one photon in the  $\mathbf{q}$ -mode is given by tracing over all possible electron final states with momentum  $\mathbf{k}_f$  and spin  $\mathbf{s}_f$  (spinor  $\mathbf{u}_f$ ):

$$|\psi_f\rangle_{\mathbf{k}_f, \mathbf{s}_f} = |\mathbf{k}_f \mathbf{s}_f; 1_{\mathbf{q}n\lambda}\rangle = |1_{\mathbf{q}n\lambda}\rangle \otimes \mathbf{u}_f(\mathbf{s}_f, \mathbf{k}_f) |\mathbf{k}_f\rangle. \quad (\text{S7})$$

Hence, the spontaneous emission rate is given as

$$w_{\mathbf{q}, n\lambda}^{sp} = \frac{t_{\text{int}}}{\hbar^2} \sum_{\mathbf{k}_f, \mathbf{s}_f} \left| \sum_{\mathbf{k}_i} \frac{\tilde{\psi}(\mathbf{k}_i)}{\sqrt{V}} \langle \mathbf{k}_f \mathbf{s}_f; 1_{\mathbf{q}n\sigma} | ec\boldsymbol{\alpha} \cdot \mathbf{A} | \mathbf{k}_i \mathbf{s}_i; 0 \rangle \text{sinc} \left[ \frac{t_{\text{int}}}{2\hbar} (E_f + \hbar\omega_{\mathbf{q}n\sigma} - E_i) \right] \right|^2 \quad (\text{S8})$$

Where  $t_{\text{int}}$  is the interaction time of the electron with the grating,  $t_{\text{int}} = L_{\text{int}}/v$ ,  $L_{\text{int}}$  is the interaction length of the electron with the grating and  $v$  is the electron velocity. We first focus on the calculation of the corresponding transition matrix elements,  $\langle \mathbf{k}_f \mathbf{s}_f; 1_{\mathbf{q}n\sigma} | ec\boldsymbol{\alpha} \cdot \mathbf{A} | \mathbf{k}_i \mathbf{s}_i; 0 \rangle$ . It is apparent that we need only keep the creation operator term in  $\mathbf{A}$  to describe spontaneous emission of SPR. First, we eliminate the action on the photon state:

$$\begin{aligned}
& \langle \mathbf{k}_f \mathbf{s}_f; 1_{\mathbf{q}n\sigma} | e c \boldsymbol{\alpha} \cdot \mathbf{A} | \mathbf{k}_i \mathbf{s}_i; 0 \rangle \\
&= ec \sqrt{\frac{\hbar}{2\epsilon_0 V \omega_{\mathbf{q}n\sigma}}} \\
&\times \left\langle \mathbf{k}_f; 1_{\mathbf{q}n\sigma} \left| a_{\mathbf{q}n\sigma}^\dagger \sum_{m=-\infty}^{\infty} \mathbf{u}_f^\dagger \boldsymbol{\alpha} \cdot \boldsymbol{\epsilon}_{m,\mathbf{q}n\sigma}^*(\mathbf{r}_T) \mathbf{u}_i A_{m,\mathbf{q}n\sigma}^*(\mathbf{r}_T) e^{-i\mathbf{q}_m \cdot \mathbf{r}} \right| \mathbf{k}_i; 0 \right\rangle \quad (\text{S9}) \\
&= ec \sqrt{\frac{\hbar}{2\epsilon_0 V \omega_{\mathbf{q}n\sigma}}} \sum_{m=-\infty}^{\infty} \langle \mathbf{k}_f | \mathbf{u}_f^\dagger \boldsymbol{\alpha} \cdot \boldsymbol{\epsilon}_{m,\mathbf{q}n\sigma}^*(\mathbf{r}_T) \mathbf{u}_i A_{m,\mathbf{q}n\sigma}^*(\mathbf{r}_T) e^{-i\mathbf{q}_m \cdot \mathbf{r}} | \mathbf{k}_i \rangle
\end{aligned}$$

Next, we compute the spinor product,  $\mathbf{u}_f^\dagger \boldsymbol{\alpha} \cdot \boldsymbol{\epsilon}_{m,\mathbf{q}n\sigma}^*(\mathbf{r}_T) \mathbf{u}_i$ . The electron recoil upon emission of the photon contributes a negligible correction to the emission amplitude, since it is an effect to first order in  $\hbar$ . It is therefore neglected for the present calculation of the spinor inner products (it is, however, important to retain the recoil in the dispersion relation, for momentum conservation). For a plane-wave electron with carrier momentum,  $\mathbf{k}_i \cong \hat{\mathbf{z}} k_{iz}$ , we have a general spin state:

$$\mathbf{u}_i = a_i \mathbf{u}_\uparrow + b_i \mathbf{u}_\downarrow, \quad \mathbf{u}_f = a_f \mathbf{u}_\uparrow + b_f \mathbf{u}_\downarrow \quad (\text{S10})$$

where

$$u_\uparrow(\mathbf{k}) = \sqrt{E + mc^2} \begin{pmatrix} 1 \\ 0 \\ \frac{\hbar c k_z}{E + mc^2} \\ 0 \end{pmatrix}, \quad u_\downarrow(\mathbf{k}) = \sqrt{E + mc^2} \begin{pmatrix} 0 \\ 1 \\ 0 \\ -\frac{\hbar c k_z}{E + mc^2} \end{pmatrix} \quad (\text{S11})$$

are the electron Dirac-spinors of each spin value. The Dirac matrices are

$$\alpha_i = \begin{pmatrix} 0 & \sigma_i \\ \sigma_i & 0 \end{pmatrix}. \quad (\text{S12})$$

where  $\sigma_i$  are the two-dimensional Pauli matrices. It can be shown that the only non-vanishing products of the form  $\mathbf{u}_{s_1}^\dagger (\boldsymbol{\alpha} \cdot \hat{\mathbf{n}}) \mathbf{u}_{s_2}$ , where  $s_1, s_2 = \uparrow, \downarrow$  and  $\hat{\mathbf{n}} = \hat{\mathbf{x}}, \hat{\mathbf{y}}, \hat{\mathbf{z}}$  are

$$\mathbf{u}_\uparrow^\dagger (\boldsymbol{\alpha} \cdot \hat{\mathbf{z}}) \mathbf{u}_\uparrow = \mathbf{u}_\downarrow^\dagger (\boldsymbol{\alpha} \cdot \hat{\mathbf{z}}) \mathbf{u}_\downarrow = 2\hbar c k_{iz} = 2p_z c \quad (\text{S13})$$

Therefore, for the spinors defined above,  $\mathbf{u}_i = a_i \mathbf{u}_\uparrow + b_i \mathbf{u}_\downarrow$ ,  $\mathbf{u}_f = a_f \mathbf{u}_\uparrow + b_f \mathbf{u}_\downarrow$  we can write

$$\mathbf{u}_f^\dagger (\boldsymbol{\alpha} \cdot \boldsymbol{\epsilon}_{m,\mathbf{q}n\sigma}^*) \mathbf{u}_i = (\hat{\mathbf{z}} \cdot \boldsymbol{\epsilon}_{m,\mathbf{q}n\sigma}^*) (a_f^* a_i + b_f^* b_i) 2p_z c = (\hat{\mathbf{z}} \cdot \boldsymbol{\epsilon}_{m,\mathbf{q}n\sigma}^*) \langle \mathbf{s}_f | \mathbf{s}_i \rangle 2p_z c \quad (\text{S14})$$

So finally we obtain:

$$\mathbf{u}_f^\dagger \boldsymbol{\alpha} \cdot \boldsymbol{\epsilon}_{m,\mathbf{q}n\sigma}^*(\mathbf{r}_T) \mathbf{u}_i = \hat{\mathbf{z}} \cdot \boldsymbol{\epsilon}_{m,\mathbf{q}n\sigma}^*(\mathbf{r}_T) \langle \mathbf{s}_f | \mathbf{s}_i \rangle 2p_z c \quad (\text{S15})$$

This gives us

$$\begin{aligned}
& \langle \mathbf{k}_f \mathbf{s}_f; 1_{\mathbf{q}n\sigma} | e c \boldsymbol{\alpha} \cdot \mathbf{A} | \mathbf{k}_i \mathbf{s}_i; 0 \rangle \\
&= 2p_z c \langle \mathbf{s}_f | \mathbf{s}_i \rangle e c \sqrt{\frac{\hbar}{2\epsilon_0 V \omega_{\mathbf{q}n\sigma}}} \\
&\quad \times \sum_{m=-\infty}^{\infty} \langle \mathbf{k}_f | \hat{\mathbf{z}} \cdot \boldsymbol{\epsilon}_{m,\mathbf{q}n\sigma}^*(\mathbf{r}_T) A_{m,\mathbf{q}n\sigma}^*(\mathbf{r}_T) e^{-i\mathbf{q}_m \cdot \mathbf{r}} | \mathbf{k}_i \rangle
\end{aligned} \tag{S16}$$

Thus, we need to evaluate a simpler matrix element (inside the sum), containing the electromagnetic mode profile:

$$\begin{aligned}
& \langle \mathbf{k}_f | \hat{\mathbf{z}} \cdot \boldsymbol{\epsilon}_{m,\mathbf{q}n\sigma}^*(\mathbf{r}_T) A_{m,\mathbf{q}n\sigma}^*(\mathbf{r}_T) e^{-i\mathbf{q}_m \cdot \mathbf{r}} | \mathbf{k}_i \rangle \\
&= \int d^3r \frac{1}{\sqrt{V}} e^{-i\mathbf{k}_f \cdot \mathbf{r}} \hat{\mathbf{z}} \cdot \boldsymbol{\epsilon}_{m,\mathbf{q}n\sigma}^*(\mathbf{r}_T) A_{m,\mathbf{q}n\sigma}^*(\mathbf{r}_T) e^{-i\mathbf{q}_m \cdot \mathbf{r}} \frac{1}{\sqrt{V}} e^{i\mathbf{k}_i \cdot \mathbf{r}} \\
&= \frac{1}{V} \int d^3r e^{-\alpha_m y} \hat{\mathbf{z}} \cdot \boldsymbol{\epsilon}_{m,\mathbf{q}n\sigma}^*(\mathbf{r}_T) A_{m,\mathbf{q}n\sigma}^*(\mathbf{r}_T) e^{i(\mathbf{k}_i - \mathbf{k}_f - q_x \hat{x} - q_z \hat{z} - \kappa_m \hat{z}) \cdot \mathbf{r}}
\end{aligned} \tag{S17}$$

Where it was assumed that the matrix element is non-vanishing only for  $m \neq 0$ , for which an evanescent field is present along the  $y$  direction  $e^{-\alpha_m y}$ . When defining the evanescent mode transverse envelope as:

$$\mathcal{E}_{m,\mathbf{q}n\sigma}(\mathbf{r}_T) \equiv e^{-\alpha_m y} \hat{\mathbf{z}} \cdot \boldsymbol{\epsilon}_{m,\mathbf{q}n\sigma}^*(\mathbf{r}_T) A_{m,\mathbf{q}n\sigma}^*(\mathbf{r}_T), \tag{S18}$$

then substituting  $\mathbf{k}_i = (\mathbf{k}_{iT}, k_{iz})$  and  $\mathbf{k}_f = (\mathbf{k}_{fT}, k_{fz})$ , the above matrix element reduces to:

$$\begin{aligned}
& \langle \mathbf{k}_f | \hat{\mathbf{z}} \cdot \boldsymbol{\epsilon}_{m,\mathbf{q}n\sigma}^*(\mathbf{r}_T) A_{m,\mathbf{q}n\sigma}^*(\mathbf{r}_T) e^{-i\mathbf{q}_m \cdot \mathbf{r}} | \mathbf{k}_i \rangle \\
&= \frac{1}{V} \delta(k_{iz} - k_{fz} - q_z - \kappa_m) \tilde{\mathcal{E}}_{m,\mathbf{q}n\sigma}(\mathbf{k}_{iT} - \mathbf{k}_{fT} - q_x \hat{x})
\end{aligned} \tag{S19}$$

With  $\tilde{\mathcal{E}}_{m,\mathbf{q}n\sigma}$  being the Fourier transform of  $\mathcal{E}_{m,\mathbf{q}n\sigma}$ . The original matrix element is found to be

$$\begin{aligned}
& \langle \mathbf{k}_f \mathbf{s}_f; 1_{\mathbf{q}n\sigma} | e c \boldsymbol{\alpha} \cdot \mathbf{A} | \mathbf{k}_i \mathbf{s}_i; 0 \rangle \\
&= 2p_z c \langle \mathbf{s}_f | \mathbf{s}_i \rangle e c \sqrt{\frac{\hbar}{2\epsilon_0 V \omega_{\mathbf{q}n\sigma}}} \\
&\quad \times \sum_{m=-\infty}^{\infty} \frac{1}{V} \delta(k_{iz} - k_{fz} - q_z - \kappa_m) \tilde{\mathcal{E}}_{m,\mathbf{q}n\sigma}(\mathbf{k}_{iT} - \mathbf{k}_{fT} - q_x \hat{x})
\end{aligned} \tag{S20}$$

We now calculate the internal sum over  $\mathbf{k}_i$  (converted to an integral below) in the Fermi golden rule, with the matrix element given above:

$$\begin{aligned}
& \sum_{\mathbf{k}_i} \frac{1}{\sqrt{V}} \tilde{\psi}(\mathbf{k}_i) \langle \mathbf{k}_f \mathbf{s}_f; 1_{\mathbf{q}n\sigma} | e c \boldsymbol{\alpha} \cdot \mathbf{A} | \mathbf{k}_i \mathbf{s}_i; 0 \rangle \text{sinc} \left[ \frac{t_{\text{int}}}{2\hbar} (E_f + \hbar\omega_{\mathbf{q}n\sigma} - E_i) \right] \\
&= \frac{1}{\sqrt{V}} 2p_z c \langle \mathbf{s}_f | \mathbf{s}_i \rangle e c \sqrt{\frac{\hbar}{2\epsilon_0 V \omega_{\mathbf{q}n\sigma}}} \sum_{m=-\infty}^{\infty} \int \frac{d^3\mathbf{k}_i}{(2\pi)^3} \tilde{\psi}(\mathbf{k}_i) \\
&\quad \times \delta(k_{iz} - k_{fz} - q_z - \kappa_m) \tilde{\mathcal{E}}_{m,\mathbf{q}n\sigma}(\mathbf{k}_{iT} - \mathbf{k}_{fT} - q_x \hat{x}) \\
&\quad \times \text{sinc} \left[ \frac{t_{\text{int}}}{2\hbar} (E_f + \hbar\omega_{\mathbf{q}n\sigma} - E_i) \right]
\end{aligned} \tag{S21}$$

The integral over  $d^3\mathbf{k}_i$  should be evaluated with all functions depending on  $\mathbf{k}_i$ . We therefore need to evaluate the argument of the sinc, using the dispersion relation (see Section D):

$$\frac{E_i - E_f}{\hbar} = \frac{\sqrt{\hbar^2 k_i^2 c^2 + m^2 c^4} - \sqrt{\hbar^2 k_f^2 c^2 + m^2 c^4}}{\hbar} \cong (\mathbf{k}_i - \mathbf{k}_f) \cdot \mathbf{v}_i \tag{S22}$$

thus

$$\omega_q - \frac{E_i - E_f}{\hbar} \cong \omega_{\mathbf{q}} - (\mathbf{k}_i - \mathbf{k}_f) \cdot \mathbf{v}_i \quad (\text{S23})$$

where we approximate  $\mathbf{v}_i = v\hat{\mathbf{z}}$  as the electron initial velocity (the carrier velocity of the paraxial wavepacket) and where the last step in the equation above is an approximation to zero order in  $\hbar$ . The paraxial approximation used here on the one hand greatly simplifies the calculation when it is employed in the dispersion relation above, while on the other hand still recovers the main results we wish to present herein. We find that, as compared to the emitted photon momentum, the paraxiality condition is  $\Delta k \ll \sqrt{qk_C}$ , where  $k_C = \frac{mc}{\hbar}$  is the Compton wavenumber for the electron and  $\Delta k$  the momentum spread of the wavepacket. Since in the SP effect we have  $q \ll k_C$ , there still exists a relatively wide regime of paraxiality even when the wavefunction momentum spread is larger than the photon momentum, i.e.  $\Delta k \gg q$ . We remark that coherent effects such as wavefunction interference [13], as well as additional SP resonances due to two-dimensional gratings, can be fully accounted for within this theory when the paraxial approximation is relaxed [14]. However, we shall leave their treatment for a future investigation.

These steps above give us for the sinc function:

$$\begin{aligned} \text{sinc} \left[ \frac{t_{\text{int}}}{2\hbar} (E_f + \hbar\omega_{\mathbf{q}\sigma} - E_i) \right] &\cong \text{sinc} \left[ \frac{t_{\text{int}}}{2} (\omega_{\mathbf{q}\sigma} - (\mathbf{k}_i - \mathbf{k}_f) \cdot \mathbf{v}_i) \right] \\ &= \text{sinc} \left[ \frac{t_{\text{int}}}{2} (\omega_{\mathbf{q}\sigma} - (k_{iz} - k_{fz})v) \right] \equiv \mathcal{G}_m(k_{iz} - k_{fz}) \end{aligned} \quad (\text{S24})$$

with  $\mathcal{G}_m$  denoting, for brevity, the grating linewidth function (the sinc function above). The integral over  $\mathbf{k}_i$  then becomes

$$\begin{aligned} &\int \frac{d^3\mathbf{k}_i}{(2\pi)^3} \tilde{\psi}(\mathbf{k}_i) \delta(k_{iz} - k_{fz} - q_z - \kappa_m) \tilde{\mathcal{E}}_{m,\mathbf{q}\sigma}(\mathbf{k}_{iT} - \mathbf{k}_{fT} - q_x\hat{\mathbf{x}}) \mathcal{G}_m(k_{iz} - k_{fz}) \\ &= \tilde{\psi}_z(k_{fz} + q_z + \kappa_m) \mathcal{G}_m(q_z + \kappa_m) \\ &\times \int \frac{d^2\mathbf{k}_{iT}}{(2\pi)^3} \tilde{\psi}_T(\mathbf{k}_{iT}) \tilde{\mathcal{E}}_{m,\mathbf{q}\sigma}(\mathbf{k}_{iT} - \mathbf{k}_{fT} - q_x\hat{\mathbf{x}}) \end{aligned} \quad (\text{S25})$$

where we integrated over the  $k_{iz}$  delta function. So the inner summation in the Fermi golden rule is

$$\begin{aligned} &\sum_{\mathbf{k}_i} \frac{1}{\sqrt{V}} \tilde{\psi}(\mathbf{k}_i) \langle \mathbf{k}_f \mathbf{s}_f; 1_{\mathbf{q}\sigma} | e c \boldsymbol{\alpha} \cdot \mathbf{A} | \mathbf{k}_i \mathbf{s}_i; 0 \rangle \text{sinc} \left[ \frac{t_{\text{int}}}{2\hbar} (E_f + \hbar\omega_{\mathbf{q}\sigma} - E_i) \right] \\ &= \frac{1}{\sqrt{V}} 2p_z c \langle \mathbf{s}_f | \mathbf{s}_i \rangle e c \sqrt{\frac{\hbar}{2\epsilon_0 V \omega_{\mathbf{q}\sigma}}} \\ &\times \sum_{m=-\infty}^{\infty} \tilde{\psi}_z(k_{fz} + q_z + \kappa_m) \mathcal{G}_m(q_z + \kappa_m) \\ &\times \int \frac{d^2\mathbf{k}_{iT}}{(2\pi)^3} \tilde{\psi}_T(\mathbf{k}_{iT}) \tilde{\mathcal{E}}_{m,\mathbf{q}\sigma}(\mathbf{k}_{iT} - \mathbf{k}_{fT} - q_x\hat{\mathbf{x}}) \end{aligned} \quad (\text{S26})$$

As the different resonances are expected to be narrow and well-separated, it is reasonable to assume that there is essentially no overlap between elements of the series for different  $m$ 's. Therefore, the summation over  $m$  can be taken to be *incoherent* when we take the absolute value of the  $m$ -sum. We then find:

$$\begin{aligned}
w_{\mathbf{q},n\sigma}^{sp} &= \frac{t_{\text{int}}}{\hbar^2} \sum_{\mathbf{k}_f, \mathbf{s}_f} \left| \sum_{\mathbf{k}_i} \frac{\tilde{\psi}(\mathbf{k}_i)}{\sqrt{V}} \langle \mathbf{k}_f \mathbf{s}_f | 1_{\mathbf{q}n\lambda} | e c \boldsymbol{\alpha} \cdot \mathbf{A} | \mathbf{k}_i \mathbf{s}_i 0 \rangle \text{sinc} \left[ \frac{t_{\text{int}}}{2\hbar} (E_f + \hbar\omega_{\mathbf{q}n\sigma} - E_i) \right] \right|^2 \\
&= (2p_z c)^2 e^2 c^2 \frac{\hbar}{2\epsilon_0 V \omega_{\mathbf{q}n\sigma}} \frac{t_{\text{int}}}{\hbar^2} \sum_{\mathbf{s}_f} |\langle \mathbf{s}_f | \mathbf{s}_i \rangle|^2 \\
&\times \sum_{m=-\infty}^{\infty} |G_m(q_z + \kappa_m)|^2 \frac{1}{V} \sum_{\mathbf{k}_f} |\tilde{\psi}_z(k_{fz} + q_z + \kappa_m)|^2 \\
&\times \left| \int \frac{d^2 \mathbf{k}_{iT}}{(2\pi)^3} \tilde{\psi}_T(\mathbf{k}_{iT}) \tilde{\mathcal{E}}_{m,\mathbf{q}n\sigma}(\mathbf{k}_{iT} - \mathbf{k}_{fT} - q_x \hat{\mathbf{x}}) \right|^2
\end{aligned} \tag{S27}$$

The spin sum  $\sum_{\mathbf{s}_f} |\langle \mathbf{s}_f | \mathbf{s}_i \rangle|^2 = \int d\Omega_s |\langle \mathbf{s}_f | \mathbf{s}_i \rangle|^2$  can be calculated by first assuming a direction of initial spin. For simplicity and without loss of generality, we assume the initial spin points in the +z direction,  $|\mathbf{s}_i\rangle = |\uparrow\rangle$ . A general spin state is given by  $|\mathbf{s}_f\rangle = \cos\frac{\theta}{2} |\uparrow\rangle + e^{i\phi} \sin\frac{\theta}{2} |\downarrow\rangle$ . So the angular integral yields

$$\int d\Omega_s |\langle \mathbf{s}_f | \mathbf{s}_i \rangle|^2 = \int d\phi \sin\theta d\theta \cos^2\frac{\theta}{2} = 2\pi \tag{S28}$$

Now we are left to replace the summation over  $\mathbf{k}_f$  with integration over  $d^3 k_f = (2\pi)^3/V$ . To correctly perform the integral over final states in phase space, we should include the Lorentz invariant phase space [15] element, due to the normalization of the Dirac spinors. We then find:

$$\begin{aligned}
&\frac{1}{2E_i} \int \frac{d^3 \mathbf{k}_f}{2E_f (2\pi)^3} |\tilde{\psi}_z(k_{fz} + q_z + \kappa_m)|^2 \left| \int \frac{d^2 \mathbf{k}_{iT}}{(2\pi)^2} \tilde{\psi}_T(\mathbf{k}_{iT}) \tilde{\mathcal{E}}_{m,\mathbf{q}n\sigma}(\mathbf{k}_{iT} - \mathbf{k}_{fT} - q_x \hat{\mathbf{x}}) \right|^2 \\
&= \frac{1}{(2E_i)^2} \int \frac{d^2 \mathbf{k}_{fT}}{(2\pi)^2} \left| \int \frac{d^2 \mathbf{k}_{iT}}{(2\pi)^2} \tilde{\psi}_T(\mathbf{k}_{iT}) \tilde{\mathcal{E}}_{m,\mathbf{q}n\sigma}(\mathbf{k}_{iT} - \mathbf{k}_{fT} - q_x \hat{\mathbf{x}}) \right|^2
\end{aligned} \tag{S29}$$

Where we approximated  $E_f \cong E_i$  and where the normalization of  $\int \frac{dk_z}{2\pi} |\tilde{\psi}_z(k_z)|^2 = 1$  was used, thus eliminating the dependence on the longitudinal part of the electron wavefunction. The last integral can be further simplified using the convolution and Parseval's theorems:

$$\begin{aligned}
&\int \frac{d^2 \mathbf{k}_{fT}}{(2\pi)^2} \left| \int \frac{d^2 \mathbf{k}_{iT}}{(2\pi)^2} \tilde{\psi}_T(\mathbf{k}_{iT}) \tilde{\mathcal{E}}_{m,\mathbf{q}n\sigma}(\mathbf{k}_{iT} - \mathbf{k}_{fT} - q_x \hat{\mathbf{x}}) \right|^2 \\
&= \int \frac{d^2 \mathbf{k}_{fT}}{(2\pi)^2} |\text{FT}\{\psi_T(\mathbf{r}_T) \mathcal{E}_{m,\mathbf{q}n\sigma}(\mathbf{r}_T)\}(\mathbf{k}_{fT} + q_x \hat{\mathbf{x}})|^2 \\
&= \int d^2 \mathbf{r}_T |\psi_T(\mathbf{r}_T)|^2 |\mathcal{E}_{m,\mathbf{q}n\sigma}(\mathbf{r}_T)|^2
\end{aligned} \tag{S30}$$

We then obtain

$$\begin{aligned}
w_{\mathbf{q},n\sigma}^{sp} &= \int d^2 \mathbf{r}_T |\psi_T(\mathbf{r}_T)|^2 \beta^2 \frac{t_{\text{int}}}{\hbar} \frac{\pi e^2 c^2}{\epsilon_0 V \omega_{\mathbf{q}n\sigma}} \sum_{m=-\infty}^{\infty} |\mathcal{E}_{m,\mathbf{q}n\sigma}(\mathbf{r}_T)|^2 \\
&\times \text{sinc}^2 \left[ \frac{t_{\text{int}}}{2} (\omega_{\mathbf{q}n\sigma} - q \cos\theta v - \kappa_m v) \right]
\end{aligned} \tag{S31}$$

where  $\beta = \frac{p_z c}{E_i}$  was used above, and  $\theta$  is the angle between  $\mathbf{q}$  and  $\hat{\mathbf{z}}$  such that  $q_z = q \cos\theta$  ( $q = |\mathbf{q}|$ ). If we approximate  $\omega_{\mathbf{q}n\sigma} \equiv \omega = cq$  and substitute the interaction time:

$$t_{\text{int}} = \frac{L_{\text{int}}}{v} = \frac{2}{\beta(\beta^{-1} - \cos \theta)} \cdot \frac{1}{\Delta\omega_{\text{int}}} \quad (\text{S32})$$

where

$$\Delta\omega_{\text{int}} = \frac{c}{\beta^{-1} - \cos \theta} \frac{2}{L_{\text{int}}} \quad (\text{S33})$$

We find:

$$w_{\mathbf{q},n\sigma}^{\text{sp}} = \int d^2\mathbf{r}_T |\psi_T(\mathbf{r}_T)|^2 \beta \frac{2\pi^2 e^2 c^2}{\epsilon_0 V \hbar \omega} \frac{1}{\beta^{-1} - \cos \theta} \times \sum_{m=-\infty}^{\infty} |\mathcal{E}_{m,\mathbf{q}n\sigma}(\mathbf{r}_T)|^2 \frac{1}{\pi \Delta\omega_{\text{int}}} \text{sinc}^2 \left[ \frac{\omega - \omega_{\text{SP},m}}{\Delta\omega_{\text{int}}} \right] \quad (\text{S34})$$

where we recall  $\omega_{\text{SP},m}$  the Smith-Purcell classical frequency,  $\omega_{\text{SP},m} = \frac{\kappa_m c}{\beta^{-1} - \cos \theta}$ . For the spectral radiant power, we have

$$\frac{d^2 P}{d\Omega d\omega} = \hbar \omega \sum_{n,\sigma} \rho_{ph}(\omega, \hat{\mathbf{q}}, n, \sigma) w_{\mathbf{q},n,\sigma}^{\text{sp}} \quad (\text{S35})$$

where  $\rho_{ph}(\omega, \hat{\mathbf{q}}, n, \sigma)$  is the density of states for the photon. The latter can be approximated by the expression for free space,  $\rho_{ph} = \frac{V \omega^2}{(2\pi)^3 c^3}$ , since we are considering modes above the light line [16]. When this is done, we find

$$\frac{d^2 P}{d\Omega d\omega} = \int d^2\mathbf{r}_T |\psi_T(\mathbf{r}_T)|^2 \frac{\hbar c^2 \alpha \beta}{(\beta^{-1} - \cos \theta)^3} \times \sum_{n\sigma} \sum_{m=-\infty}^{\infty} \kappa_m^2 |\mathcal{E}_{m,\mathbf{q}n\sigma}(\mathbf{r}_T)|^2 \frac{\text{sinc}^2 \left[ \frac{\omega - \omega_{\text{SP},m}}{\Delta\omega_{\text{int}}} \right]}{\pi \Delta\omega_{\text{int}}} \quad (\text{S36})$$

where  $\alpha = \frac{e^2}{4\pi\epsilon_0 \hbar c}$  is the fine structure constant. For a very localized particle,  $|\psi_T|^2$  is a delta function centered about some  $\mathbf{r}_T = \mathbf{r}_0$ , and we recover the "classical" result which is dependent on the specific *location*  $\mathbf{r}_0$  of the electron within the evanescent mode:

$$\frac{d^2 P^{\text{class}}}{d\Omega d\omega}(\mathbf{r}_0) = \frac{\hbar c^2 \alpha \beta}{(\beta^{-1} - \cos \theta)^3} \sum_{n\sigma} \sum_{m=-\infty}^{\infty} \kappa_m^2 |\mathcal{E}_{m,\mathbf{q}n\sigma}(\mathbf{r}_0)|^2 \frac{\text{sinc}^2 \left[ \frac{\omega - \omega_{\text{SP},m}}{\Delta\omega_{\text{int}}} \right]}{\pi \Delta\omega_{\text{int}}} \quad (\text{S37})$$

with

$$|\mathcal{E}_{m,\mathbf{q}n\sigma}(\mathbf{r}_0)|^2 = e^{-2\alpha_{m\gamma}} |\hat{\mathbf{z}} \cdot \hat{\mathbf{e}}_{m,\mathbf{q}n\sigma}^*(\mathbf{r}_0) A_{m,\mathbf{q}n\sigma}^*(\mathbf{r}_0)|^2 \quad (\text{S38})$$

containing the familiar exponential decay away from the grating plane, in addition to an implicit dependence on the angle  $\theta$ , which must be numerically evaluated. Its limiting case, where  $\hat{\mathbf{e}}_{m,\mathbf{q}n\sigma}$  coincides with the polarization of the far field radiation, should recover the usual dipole radiation pattern of  $\sin^2 \theta$  (as in the classical approach of surface currents). Remarkably, we can express the *fully quantum* result of the spontaneous emission pattern when  $|\psi_T|^2$  is different than a delta function in terms of the "classical" result

$$\frac{d^2 P^{\text{quant}}}{d\Omega d\omega} = \int d^2\mathbf{r}_T |\psi_T(\mathbf{r}_T)|^2 \frac{d^2 P^{\text{class}}}{d\Omega d\omega}(\mathbf{r}_T) \quad (\text{S39})$$

We remark that despite the fact that we are eventually considering the far-field radiation, it is not in general true that the photon density of states  $\rho_{ph}(\omega, \hat{\mathbf{q}}, \sigma)$  equals the free space value, since the original modes were assumed to be Bloch modes induced by the periodic grating boundary condition [16,17]. For example, if the density of states for the Bloch modes is polarization-dependent, then an angular dependence is expected to appear in  $\rho_{ph}$ , as well as in the final emission pattern. However, the emission pattern we derived is quite general and holds for an arbitrary paraxial envelope for the electron. Ignoring exotic circumstances in which the photonic density of states is localized in the continuum [18–20], it is reasonable to assume that  $\rho_{ph}$  is well-behaved and not sharply peaked around a certain direction in space. Thus, all our conclusions are still expected to hold.

#### D. The Smith-Purcell dispersion relations

This section derives the Smith-Purcell dispersion relation from conservation laws and emphasizes the important role of the paraxial approximation we take throughout the paper.

##### Taylor expansion of the dispersion relation

We compute here the Taylor expansion of the SP dispersion:

$$\frac{E_i - E_f}{\hbar} \cong (\mathbf{k}_i - \mathbf{k}_f) \cdot \mathbf{v}_i + \frac{1}{2} \frac{\hbar}{mc^2 \gamma_i} \left\{ [(\mathbf{k}_i - \mathbf{k}_f) \cdot \mathbf{v}_i]^2 - c^2 (\mathbf{k}_i - \mathbf{k}_f)^2 \right\} \quad (\text{S40})$$

First, let us write

$$\frac{E_i - E_f}{\hbar} = c \left( \sqrt{k_i^2 + \frac{m^2 c^2}{\hbar^2}} - \sqrt{k_f^2 + \frac{m^2 c^2}{\hbar^2}} \right) \quad (\text{S41})$$

Define  $k_c^2 = \frac{m^2 c^2}{\hbar^2}$  as the Compton wave vector and write

$$\begin{aligned} \frac{E_i - E_f}{\hbar} &= c \left( \sqrt{k_i^2 + k_c^2} - \sqrt{(\mathbf{k}_f - \mathbf{k}_i) \cdot (\mathbf{k}_f + \mathbf{k}_i) + k_i^2 + k_c^2} \right) \\ &= c \sqrt{k_i^2 + k_c^2} \left( 1 - \sqrt{1 - \frac{(\mathbf{k}_i - \mathbf{k}_f) \cdot 2\mathbf{k}_i - (\mathbf{k}_i - \mathbf{k}_f)^2}{k_i^2 + k_c^2}} \right) \end{aligned} \quad (\text{S42})$$

Now use  $\sqrt{1+x} \cong 1 + \frac{x}{2} - \frac{x^2}{8}$  to expand up to  $(\mathbf{k}_i - \mathbf{k}_f)^2$ :

$$\begin{aligned} \frac{E_i - E_f}{\hbar} &\cong c \sqrt{k_i^2 + k_c^2} \left( \frac{(\mathbf{k}_i - \mathbf{k}_f) \cdot \mathbf{k}_i}{k_i^2 + k_c^2} - \frac{1}{2} \frac{(\mathbf{k}_i - \mathbf{k}_f)^2}{k_i^2 + k_c^2} + \frac{[(\mathbf{k}_i - \mathbf{k}_f) \cdot \mathbf{k}_i]^2}{2(k_i^2 + k_c^2)^2} \right) \\ &= \frac{c(\mathbf{k}_i - \mathbf{k}_f) \cdot \mathbf{k}_i}{\sqrt{k_i^2 + k_c^2}} \left( 1 + \frac{1}{2} \frac{(\mathbf{k}_i - \mathbf{k}_f) \cdot \mathbf{k}_i}{k_i^2 + k_c^2} \right) - \frac{1}{2} \frac{c(\mathbf{k}_i - \mathbf{k}_f)^2}{\sqrt{k_i^2 + k_c^2}} \end{aligned} \quad (\text{S43})$$

Now divide and multiply by  $\hbar c$  or  $\hbar^3 c^3$  and use  $E_i = \hbar c \sqrt{k_i^2 + k_c^2}$ ,  $\gamma = \frac{E}{mc^2}$  and  $v = pc/E$  to obtain:

$$\frac{E_i - E_f}{\hbar} = \frac{\hbar}{m\gamma_i} (\mathbf{k}_i - \mathbf{k}_f) \cdot \mathbf{k}_i \left( 1 + \frac{\hbar^2}{2m^2 c^2 \gamma_i^2} (\mathbf{k}_i - \mathbf{k}_f) \cdot \mathbf{k}_i \right) - \frac{\hbar}{2m\gamma_i} (\mathbf{k}_i - \mathbf{k}_f)^2 \quad (\text{S44})$$

Reordering recovers Eq. (S40).

The slowly-varying envelope approximation for the dispersion equation and the effect of transverse momentum of the grating

The SP dispersion relation to zero-order in  $\hbar$  is

$$\omega_{\mathbf{q}} - (\mathbf{k}_i - \mathbf{k}_f) \cdot \mathbf{v}_i = 0 \quad (\text{S45})$$

This relation can be further approximated to simplify the calculations. For this aim we employ the SVE approximation for the incoming electron, which assumes a carrier wave vector  $\mathbf{k}_{i0} = k_{i0} \hat{\mathbf{z}}$  such that

$$\mathbf{k}_i = \mathbf{k}_{i0} + \delta\mathbf{k}_i, \quad |\delta\mathbf{k}_i| \ll k_{i0} \quad (\text{S46})$$

We expand the dispersion in the small vector  $\delta\mathbf{k}_i$  (for a given  $\mathbf{k}_f$ ) as:

$$\omega - (\mathbf{k}_i - \mathbf{k}_f) \cdot \mathbf{v}_i = \omega - (\mathbf{k}_i - \mathbf{k}_f) \cdot \mathbf{v}_{i0} - \Theta(\mathbf{k}_i - \mathbf{k}_f) \cdot \widehat{\delta\mathbf{k}}_i v_{i0} \quad (\text{S47})$$

where  $\mathbf{v}_{i0}$  is the carrier initial velocity,  $\Theta = \delta k/k_{i0}$  is the relative magnitude of the paraxial correction, and  $\widehat{\delta\mathbf{k}}_i$  the direction of this correction. In the derivation we used so far, we neglected the  $\Theta$  term, and this approximation holds when it is negligible compared to the interaction linewidth:

$$\Theta(\mathbf{k}_i - \mathbf{k}_f) \cdot \widehat{\delta\mathbf{k}}_i v_{i0} \ll \Delta\omega_{\text{int}} \quad (\text{S48})$$

where  $\Delta\omega_{\text{int}} = \frac{c}{\beta^{-1} - \cos\theta} \frac{2}{L_{\text{int}}}$ , becoming smallest for  $\theta = \frac{\pi}{2}$ , for which  $\Delta\omega_{\text{int}} = \frac{2v_{i0}}{L_{\text{int}}}$ . From momentum conservation we have  $\mathbf{k}_i - \mathbf{k}_f = \mathbf{q} + \boldsymbol{\kappa}_z + \boldsymbol{\kappa}_T$ , where  $\boldsymbol{\kappa}_z$  and  $\boldsymbol{\kappa}_T$  are the additional longitudinal and transverse momenta of the grating, respectively, where the latter occurs for 2D gratings (or tilted 1D gratings). Paraxial corrections  $\Theta\widehat{\delta\mathbf{k}}_i$  can be resolved from the carrier emission line whenever:

$$\Theta \sim \frac{2}{L_{\text{int}}(q + \kappa)} \quad (\text{S49})$$

where  $\kappa$  stands for either  $\kappa_T$  or  $\kappa_z$ . This imposes an explicit condition for the SVE approximation in terms of the electron momentum uncertainty  $\Delta k$ :

$$\Theta = \frac{\Delta k}{k_{i0}} \ll \frac{1}{\pi} \frac{\lambda_{\text{ph}}}{L_{\text{int}}} \frac{\Lambda}{\Lambda + \lambda_{\text{ph}}} \quad (\text{S50})$$

As an example, for a transverse period of  $\Lambda = 100$  nm, photon wavelength  $\lambda_{\text{ph}} = 500$  nm and interaction length  $L_{\text{int}} = 10 \mu\text{m}$  we find  $\theta \ll 3$  mrad. Although higher orders in SP transverse contributions can become significant even for large  $\Lambda$ , their amplitude becomes smaller accordingly.

Smith Purcell radiation at conditions in which the contribution of the transverse momentum becomes non-negligible opens a new regime that while still being paraxial for the electron propagation, may alter the Smith-Purcell emission profile due to interference with the 2D grating.

## References

1. L. Reimer and H. (Helmut) Kohl, *Transmission Electron Microscopy: Physics of Image Formation* (Springer, 2008).
2. B. Cho, T. Ichimura, R. Shimizu, and C. Oshima, "Quantitative Evaluation of Spatial Coherence of the Electron Beam from Low Temperature Field Emitters," *Phys. Rev. Lett.* **92**, 246103 (2004).
3. B. Cho and C. Oshima, "Electron beam coherency determined from interferograms of carbon nanotubes," *Bull. Korean Chem. Soc.* **34**, 892–898 (2013).

4. T. Latychevskaia, "Spatial coherence of electron beams from field emitters and its effect on the resolution of imaged objects," *Ultramicroscopy* **175**, 121–129 (2017).
5. R. Shiloh, Y. Lereah, Y. Lilach, and A. Arie, "Sculpturing the electron wave function using nanoscale phase masks," *Ultramicroscopy* **144**, 26–31 (2014).
6. N. Voloch-Bloch, Y. Lereah, Y. Lilach, A. Gover, and A. Arie, "Generation of electron Airy beams," *Nature* **494**, 331–335 (2013).
7. R. Shiloh, Y. Tsur, R. Remez, Y. Lereah, B. A. Malomed, V. Shvedov, C. Hnatovsky, W. Krolikowski, and A. Arie, "Unveiling the Orbital Angular Momentum and Acceleration of Electron Beams," *Phys. Rev. Lett.* **114**, 096102 (2015).
8. H. Lichte and M. Lehmann, "Electron holography—basics and applications," *Reports Prog. Phys.* **71**, 016102 (2008).
9. J. C. H. Spence, W. Qian, and M. P. Silverman, "Electron source brightness and degeneracy from Fresnel fringes in field emission point projection microscopy," *J. Vac. Sci. Technol. A Vacuum, Surfaces, Film.* **12**, 542–547 (1994).
10. G. Pozzi, "Theoretical considerations on the spatial coherence in field emission electron microscope," *Optik (Stuttg.)* **7**, 69–73 (1987).
11. S. J. Glass and H. Mendlowitz, "Quantum Theory of the Smith-Purcell Experiment," *Phys. Rev.* **174**, 57–61 (1968).
12. A. Friedman, A. Gover, G. Kurizki, S. Ruschin, and A. Yariv, "Spontaneous and stimulated emission from quasifree electrons," *Rev. Mod. Phys.* **60**, 471–535 (1988).
13. C. Murdia, N. Rivera, T. Christensen, L. J. Wong, J. D. Joannopoulos, M. Soljačić, and I. Kaminer, "Controlling light emission with electron wave interference," (2017).
14. C. Kremers, D. N. Chigrin, and J. Kroha, "Theory of Cherenkov radiation in periodic dielectric media: Emission spectrum," *Phys. Rev. A* **79**, 1–10 (2009).
15. M. E. Peskin and D. V. Schroeder, *An Introduction To Quantum Field Theory*. (Westview Press, 1995).
16. J. D. Joannopoulos, S. G. Johnson, J. N. Winn, and R. D. Meade, *Photonic Crystals: Molding the Flow of Light (Second Edition)*. (Princeton University Press, 2008).
17. C. Luo, M. Ibanescu, S. G. Johnson, and J. D. Joannopoulos, *Cerenkov Radiation in Photonic Crystals* (n.d.).
18. C. W. Hsu, B. Zhen, A. D. Stone, J. D. Joannopoulos, and M. Soljačić, "Bound states in the continuum," *Nat. Rev. Mater.* **1**, 16048 (2016).
19. B. Zhen, C. W. Hsu, Y. Igarashi, L. Lu, I. Kaminer, A. Pick, S.-L. Chua, J. D. Joannopoulos, and M. Soljačić, "Spawning rings of exceptional points out of Dirac cones," *Nature* **525**, 354–358 (2015).
20. C. W. Hsu, B. Zhen, J. Lee, S.-L. Chua, S. G. Johnson, J. D. Joannopoulos, and M. Soljačić,

"Observation of trapped light within the radiation continuum," *Nature* **499**, 188–191 (2013).